Bulletin of the Seismological Society of America, Vol. 92, No. 2, pp. 570–580, March 2002

Accelerating Seismic Crustal Deformation in the Southern Aegean Area

by C. B. Papazachos, G. F. Karakaisis, A. S. Savvaidis, and B. C. Papazachos

Abstract A region of intense accelerating seismic crustal deformation has been identified in the southwestern part of the Hellenic arc (broader area of Cythera island). The identification is performed using a detailed parametric grid search of the broader southern Aegean area for accelerating energy release behavior. The identified region has similar properties with past preshock (critical) regions, which have been identified for strong mainshocks in the Aegean area. Based on such observations, which suggest that this region is at a critical state that can lead to a critical point, that is, to the generation of a mainshock, an estimation is made of the possible epicenter coordinates, magnitude, and origin time of this oncoming large (**M** ~7.0) earthquake. The estimation procedure is validated on the basis of retrospective analysis of strong events in the Aegean area, as well as by appropriate application on synthetic random catalogs. These results, the existence of similar observations of accelerating seismic deformation in eastern part of southern Aegean and independent information on the time distribution of large earthquakes (**M** ≥6.8) for the whole southern Aegean indicate that the generation of strong earthquakes in this area in the next few years must be considered as very probable.

Introduction

The southern Aegean (34° N–38.5° N, 19° E–30° E) is seismically one of the most active parts of western Eurasia (Fig. 1). The most dominant feature of the area is the Hellenic trench, where subduction of the eastern Mediterranean lithosphere (front part of the African lithospheric plate) takes place under the Aegean microplate. To the north of the trench, the sedimentary part of the Hellenic arc (Peloponnesus–Cythera–Crete–Rhodes) represents the accretionary prism. Moving farther north we can identify the other typical elements of a subduction system, namely the southern Aegean trough (sea of Crete) and the volcanic arc (Sousaki, Methana, Milos, Santorini, and Nisyros). Shallow- and intermediate-depth earthquakes with magnitudes up to about 8.0 have occurred in this area (e.g., Papazachos, 1990). The main geotectonic features of the southern Aegean are shown in Figure 1, whereas the inset in Figure 1 shows the broader area with the solid-line box delineating the investigated area.

During the time period 1948–1957 four shallow mainshocks with magnitudes 7.1 (9.2.1948, 35.5° N–27.2° E), 7.0 (17.12.1952, 34.4° N–24.5° E), 7.5 (9.7.1956, 36.6° N–26.0° E) and 7.2 (25.4.1957, 36.5° N–28.8° E) occurred in this area (magnitudes reported hereafter are moment magnitudes or equivalent moment magnitudes, following Papazachos *et al.* [1999]). Before all these mainshocks, accelerating intermediate magnitude seismicity (typically in the range **M** 4.5–6.0) was observed (B. C. Papazachos and C. B. Papazachos, 2000; C. B. Papazachos and B. C. Papazachos, 2000). A similar accelerating seismicity release pattern that has started several years ago is currently observed in southern Aegean and is the main factor that motivated the present study. An additional factor is the lack of generation of strong earthquakes in the entire southern Aegean in the past several years (Papazachos and Papazachou, 1997).

Observations on accelerating intermediate magnitude seismicity have been reported during the last 40 yr by various researchers (e.g., Tocher, 1959; Mogi, 1969; Sykes and Jaume, 1990; Knopoff *et al.,* 1996). However, during the last decade the related research efforts have been intensified, as it has been realized that the process of generation of intermediate magnitude shocks (preshocks) can be considered as a critical phenomenon and the largest earthquake (mainshock) as a critical point (e.g., Sornette and Sornette, 1990; Sornette and Sammis, 1995; Huang *et al.,* 1998; Jaume and Sykes, 1999). By the term intermediate magnitude we usually indicate seismicity around 2–3 magnitude units less than the mainshock magnitude (Jaume and Sykes, 1999). A consequence of this concept is that the time variation of measures of preshock–mainshock seismic crustal deformation (seismic energy, seismic moment, Benioff strain) follows a power law. Based on this law, Bufe and Varnes (1993) proposed the so-called time-to-failure method, which has been used in several attempts to predict earthquakes (Varnes, 1989; Sornette and Sammis, 1995; Bufe *et al.,* 1994). Bowman *et al.* (1998) proposed an algorithm to quantify the accelerating seismic energy release (specifically Benioff strain) by minimizing a curvature parameter, *C*, which is defined as

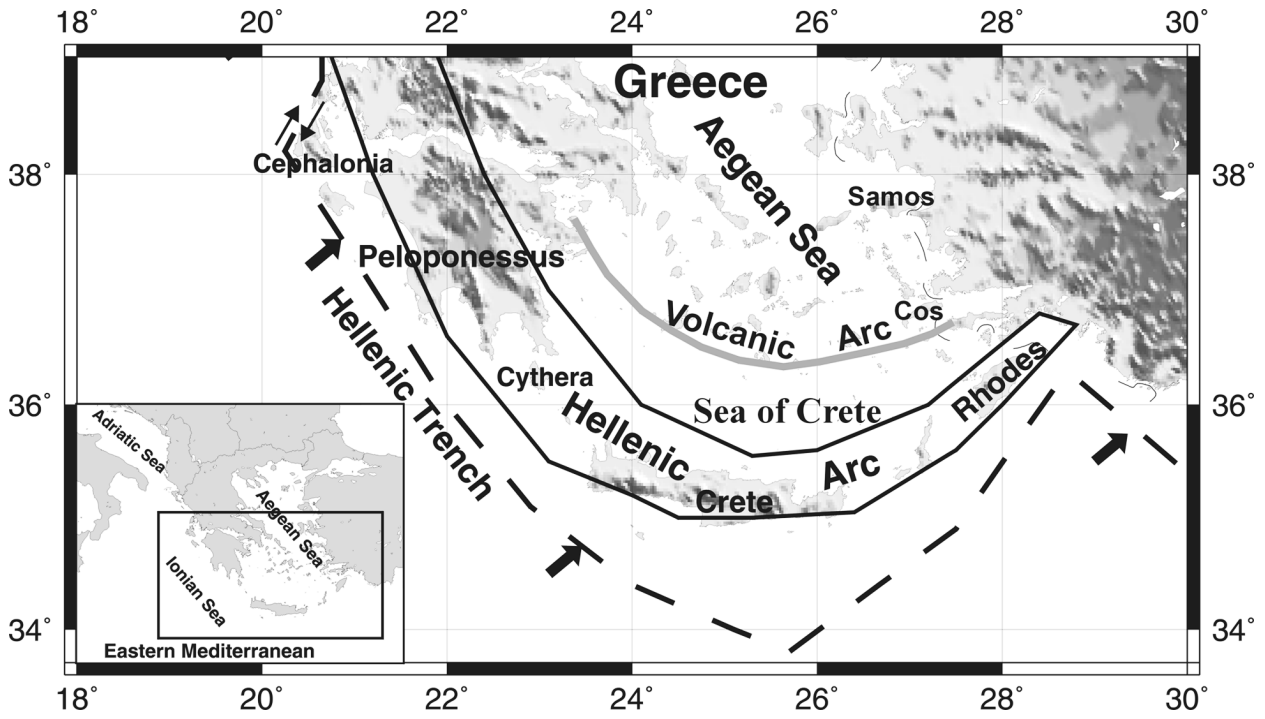

Figure 1. Main geotectonic features of the southern Aegean area. The inset figures shows the western broader Mediterranean area with the study area denoted by the rectangle.

the ratio of the root-mean-square error of the power-law fit to the corresponding linear fit error. Thus, C is quite less than 1 for accelerating ($m < 1$) or decelerating ($m > 1$) seismicity release and almost equal to 1 for a steady (linear) variation of seismicity with time. In practice, we are only interested in accelerating seismicity release, therefore m is constrained to be less than 1, in which case C is quite smaller than 1 only for accelerating seismic deformation.

Some observations on preshock accelerating seismicity in the Aegean area have already been made by various researchers (Papadopoulos, 1986, Karakaisis *et al.,* 1991; Tzanis *et al.,* 2000). During the last 2 yr systematic work has been carried out to define several semiempirical relations concerning the model of accelerated preshock seismic deformation using data for shallow earthquakes in the Aegean area (B. C. Papazachos and C. B. Papazachos, 2000; Papazachos *et al.,* 2000b; Papazachos and Papazachos, 2001). On the basis of these relations of the time-to-failure power-law (Bufe and Varnes, 1993) and using the curvature parameter (Bowman *et al.,* 1998) an algorithm has been developed to identify elliptical regions of accelerating deformation and for future earthquake prediction. This algorithm has already been tested retrospectively for a large set of earthquakes that have already occurred in the broader Aegean area (Papazachos *et al.,* 2002). The purpose of the present work is to examine the time variation of seismic energy release in the southern Aegean and to attempt to identify regions of accelerating deformation in order to estimate the main parameters (epicenter, magnitude, and origin time) of the ensuing earthquake or earthquakes in this area. The application of the models of accelerating deformation prior to large events in a predictive manner relies on the similarity of the properties of the identified preshock region with the corresponding preshock regions of past events in the area and on appropriate significance testing on synthetic random catalogs.

Background

Bufe and Varnes (1993) used the cumulative Benioff strain, $S(t)$, as a measure of the preshock seismic deformation at time, t, defined as:

$$S(t) = \sum_{i=1}^{n(t)} E_i(t)^{1/2}, \tag{1}$$

where E_i is the seismic energy of the ith preshock and $n(t)$ is the number of events that have occurred up to time t. For the time variation of the cumulative Benioff strain they have proposed a relation of the form:

$$S(t) = A + B(t_c - t)^m, \tag{2}$$

where t_c is the origin time of the mainshock and A, B, and m are parameters that can be calculated by the available observations. Seismic energy is usually calculated from the corresponding magnitude of the earthquakes. Instead of the

Benioff strain (roughly proportional to $E^{1/2}$), other measures, such as the seismic moment ($\sim E^1$) or the number of events ($\sim E^0$), have been used to describe such accelerating behavior phenomena. In the present work we selected to use the term *accelerating seismic crustal deformation* in order to reflect the physical process that takes place at the critical preshock area.

Papazachos and Papazachos (B. C. Papazachos and C. B. Papazachos, 2000; C. B. Papazachos and B. C. Papazachos, 2000, 2001) studied the preshock behavior of large earthquakes in the Aegean area and defined several relations, which can be used as additional constraints for the model expressed by equation (2). Thus, they used elliptical rather than circular regions around the epicenter of each considered mainshock by applying a large range of ellipticities (typically 0., 0.5, 0.6, 0.7, 0.8, 0.9, and 0.95) and ellipse azimuths (in steps of 10°–20°) in their parametric scan. Their results show that the following three relations apply between the magnitude, M, of the mainshock and (1) the radius, R (in km), of the circle with area equal to the area of the critical elliptical region, (2) the parameter B of equation (2) and, (3) the average magnitude, M_{13}, of the three largest preshocks:

$$\log R = 0.41\,M - 0.64, \quad \sigma = 0.05, \tag{3}$$

$$\log B = 0.64\,M + 3.27, \quad \sigma = 0.16, \tag{4}$$

$$M = 0.85\,M_{13} + 1.52, \quad \sigma = 0.21. \tag{5}$$

Similarly, the following two constraints can be applied for the determination of the duration, t_p (in yr), of the preshock sequence:

$$\log t_p = 5.81 - 0.75 \log s_r, \quad \sigma = 0.17, \tag{6}$$

$$A = S_r\ t_p, \tag{7}$$

where S_r (in joule$^{1/2}$/yr) is the long-term Benioff strain rate, expressing the average strain energy release in the examined area, and s_r is the same quantity reduced to the area of 10^4 km^2 in order to express the average seismicity rate for each examined area.

In all calculations the values of the parameter m of equation (2) and of the curvature parameter, C, are initially constrained to be smaller than 0.7, when the center of the elliptical critical region coincides with the mainshock epicenter. That is,

$$m \le 0.7, \quad C \le 0.7. \tag{8}$$

The small C-values ensure that the accelerated seismicity law (equation 2) describes the data much more adequately (smaller root mean square [rms]) than the standard linear time variation in order to avoid misidentifications. On the other hand, m-values larger than 0.7 result in a time variation that is practically indistinguishable from the linear variation.

To quantify the compatibility of the values of the parameters R, t_p, A, B, and m calculated for a seismic sequence with those determined by equations (3)–(7), a parameter P was defined (Papazachos and Papazachos, 2001a), which is the sum of probabilities calculated for each of the left-side parameters in these equations, assuming that the observed deviations of each parameter follow a Gaussian distribution. Furthermore, we have chosen the quantity $q = P/(mC)$ as a measure of the quality of each solution. The quantity q is an empirical attempt to simultaneously evaluate (1) the compatibility of an identification of accelerated seismic deformation with the behavior of past strong mainshocks (large P), (2) the deviation of seismic deformation from linearity (small C) and, (3) the degree of nonlinearity of the seismic deformation behavior (small m). Using P and q as additional criteria for strong earthquakes in the Aegean area since 1950 and considering as centers of the elliptical critical region not only the mainshock epicenters but also neighboring points resulted in the following cutoff values:

$$C \le 0.6, \quad m \le 0.4, \quad P \ge 0.4, \quad q \ge 3.5, \tag{9}$$

while the corresponding average values were $[C] = 0.44 \pm 0.12$, $[m] = 0.29 \pm 0.06$, $[P] = 0.53 \pm 0.07$, and $[q] = 4.9 \pm 2.1$.

The accelerating seismic deformation behavior, following all equations previously determined could not be identified (in accordance with the criteria defined in equation 8) until a time, t_i, before the occurrence of the mainshock, which can be described as the identification time for this phenomenon. Papazachos *et al.* (2001) showed that the difference $\Delta t_{ci} = t_c - t_i$ between the identification time and the origin time of the mainshock is of the order of several years (3.7 ± 1.6 yr) and is given by the equation:

$$\log(t_c - t_i) = 5.04 - 0.75 \log s_r, \quad \sigma = 0.18; \tag{10}$$

hence, the identification period is larger for low-seismicity areas. The curvature parameter, C, has large values (>0.60) at the identification time and gradually decreases as we approach the origin time of the mainshock. Comparing equation (10) with equation (6) shows that the time difference between the origin time of the mainshock and the identification time is given by the following equation:

$$t_c - t_i = (0.17 \pm 0.05)\, t_p. \tag{11}$$

Equation (11) suggests that the identification period represents 10%–20% of the total preshock time before a large shock. In other words, the constraints imposed by equations (3)–(8), as well as the pattern of seismic energy release, do not allow the identification of the accelerated seismic strain release until we are quite close to the mainshock. The identification period defined by equation (11) is almost identical to the results derived independently by Yang *et al.* (2001),

using an alternative approach proposed by Vere-Jones *et al.* (2001), which suggests that only when we reach the final one-sixth (~17%) of the total preshock window can the preshock region be identified. This is an advantageous feature of this phenomenon as equations (10) and (11) can be used to further constrain the origin time of an oncoming mainshock, since s_r and t_p can be estimated by the available data at the identification time.

Method and Data

To apply this method for identification of preshock (critical) regions, an algorithm developed by Papazachos and Papazachos (2001) was used. According to this algorithm, shocks (preshocks) with epicenters in the elliptical region centered at a certain point (epicenter of a mainshock or assumed epicenter of an oncoming mainshock) are considered, and the parameters of equation (2) and the curvature parameter, C, are calculated. Calculations are repeated by applying a systematic search of a large set of values for the azimuth, z, of the large ellipse axis, its length, a, ellipticity, e, and the time, t_p, since accelerating seismic deformation started. These calculations are repeated by considering several magnitudes (ranging typically from M_{start} 6.0 to the magnitude of the largest known earthquake in the area, M_{max}) and several origin times for the assumed future mainshock. These computations are repeated for a grid of points in which the investigated area is separated with the desired density. From all solutions obtained, the one that fulfills equations (2)–(9) and has the smallest q parameter is chosen as the best solution. The selected grid point and the corresponding magnitude and origin time are considered as the epicenter, magnitude, and origin time, respectively, of the oncoming mainshock. However, the finally adopted magnitude value is the average of the values calculated by equations (3)–(5).

Application of the previously described procedure for retrospective prediction of strong mainshocks that already occurred in the Aegean area has shown that this procedure gives satisfactory results for the epicenter and magnitude but only a rough estimation of the probable origin time. For this reason an alternative technique has been proposed and tested for the determination of the origin time. This technique is based on a precursory seismic excitation, which has been observed to occur in the preshock region at a time that is correlated to the origin time of the oncoming mainshock (Papazachos *et al.,* 2001). The identification of this seismic excitation has been recognized by the following procedure: For several future assumed origin times, T_c, of the mainshock, the corresponding identification times, T_i, are calculated. All calculations are made with data concerning preshocks that occur in the critical region between the start of preshock sequence and the time T_i. An abrupt change (jump) of T_i is observed in the $T_i = f(T_c)$ equation where T_c is about equal to the origin time, t_c, of the mainshock. This abrupt increase of T_i at $T_c \simeq t_c$ has been attributed to a seismic excitation in the preshock region at a time T_i that corresponds to $T_c \simeq t_c$ The suggestion that this increase of T_i is caused by a seismic excitation (swarm of events, etc.) is strongly supported by the observation that this increase is associated with variations of the other parameters that are expected to change due to a seismic excitation. Such changes are the increase of the frequency of preshocks, n, and the decrease of the curvature parameter, C, of the power-law exponent, m, and of the difference, t_{13}, between the mean origin time of the three largest preshocks and the mainshock. The decrease of C and m is explained by the additional deviation from linearity of $S(t)$ caused by the seismic excitation, whereas the decrease of t_{13} is due to the occurrence of at least one of the three largest preshocks during this excitation.

These observations have shown that changes in these five parameters (positive for T_i and n and negative for C, m, and t_{13}) can be used as measures of the seismic excitation. Thus, considering the relative rate for each parameter (e.g., the ratio of its rate to the maximum absolute value of the rate observed during the whole examined period), a measure of the seismic excitation expressed in terms of these five ratios (r_i, r_n, r_c, r_m, r_t) is calculated for each time interval in which the examined period is separated. The average of the five relative values is considered as such measure and is called the preshock excitation indicator (PEI). Its values vary between 0 and 1 for relative increase of the seismic activity (seismic excitation) with respect to the activity predicted by equation (2) and between -1 and 0 for relative decrease of seismic activity (seismic quiescence).

Papazachos *et al.* (2001) calculated the function PEI(T_c) for 32 strong mainshocks ($\mathbf{M} \geq 6.0$) that occurred in the Aegean area since 1947 (for periods of 5 yr and in steps of 3 months). They found that in 30 of these cases there is a pronounced positive value of PEI that occurred at a certain time T_{pr} corresponding to approximately t_c. The average of these maximum PEI values are found equal to 0.48 ± 0.28, indicating a statistically significant positive value, namely, a pronounced seismic excitation. The mean difference between the observed origin times, t_c, of these 30 events and the corresponding T_{pr} times is almost 0 with a standard deviation of 0.9 yr, quite smaller than the equivalent standard deviation for the random (uniform) distribution corresponding to the 5-yr examined period. Hence, this precursory excitation is recognizable and can be used to narrow the accuracy of the origin time estimation of an ensuing mainshock. The two cases where no excitation was observed correspond to a fixed value for T_i (no change for different values of T_c). This value of T_i can be used in equation (11) for an estimation of the origin time.

The data used in the present study to calculate the Benioff strain have been taken from the catalog of Papazachos *et al.* (2000a) and belong to one of the following three complete sets of shocks: 1911–1949, $\mathbf{M} \geq 5.2$; 1950–1964, $\mathbf{M} \geq 5.0$; 1965–2000, $\mathbf{M} \geq 4.5$ with focal depths $h \leq 100$ km. The errors in the epicenters are of the order of 15–20 km for earthquakes that occurred after 1965 (when the first network

of seismic stations was established in Greece) and up to 25–30 km for older earthquakes. All magnitudes are equivalent moment magnitudes and their errors are up to 0.3. The equation

$$\log E = 1.5\mathbf{M} + 4.7 \tag{12}$$

derived by B. C. Papazachos and C. B. Papazachos (2000) has been used to calculate the seismic energy from the moment magnitude, whereas the Benioff strain is calculated by equation (1).

Results for the Southern Aegean Area

Following the previously described procedure, the broader southern Aegean area (34° N–38.5° N, 19° E–30° E) has been separated in a dense grid with a spacing of 0.25° × 0.25°. For each point if more than one solutions were available we have adopted the highest q solution as the best choice. Figure 2 shows the final spatial distribution of the *C, m, P,* and q-values using this approach. A large area of very low C- and m-values and high P- and q-values can be observed in the southwestern part of the examined area. The geometrical center of the area where q obtains its largest values is located in the Cythera area, which can be considered as the epicentral area of an oncoming mainshock. Moreover, the solution parameters (z, a, e, t_p, m, A, B, etc.) that have been recomputed and correspond to the center of this maximum q area, as well as $\mathbf{M}$ and t_c corresponding to this best solution, can be adopted as the model parameters, magnitude, and origin time of the future mainshock.

The finally adopted solution is presented in the first line of Table 1, where the predicted epicenter coordinates (ϕ, λ), its magnitude ($\mathbf{M}$), origin time (t_c), curvature parameter (C), parameter (m), quality factor (q), length of the large ellipse axis (a) (in km), its azimuth (z), and ellipticity (e) are given. The minimum magnitude considered for the preshocks ($M_{\min}$), the number (n) of observations (number of preshocks including the mainshock) and the year (t_s) since the accelerating preshock deformation started ($t_{\text{mainshock}} - t_p$), and the value of PEI are also presented. Note that the solution presented in Table 1 is quite insensitive to $M_{\min}$. We have tested various values for $M_{\min}$ (e.g., 4.5, 5.0) following Jaume and Sykes's (1999) idea about the minimum cutoff magnitude and obtained very similar results. Use of a much smaller $M_{\min}$ value (~4.0) results in solutions of much poorer quality (larger C- and m-values, etc.), similar to the observation made by B. C. Papazachos and C. B. Papazachos (2000) for accelerating seismic deformation before mainshocks of the same order of magnitude (~7.0).

Figure 3 presents the finally adopted elliptical critical region in the western part of southern Aegean and the preshock epicenters for which magnitudes were used to calculate the cumulative Benioff strain, S, as well as the proposed center of the preshock area, which is denoted by a star. Comparing the elliptical region of Figure 3 with Figure 2 shows

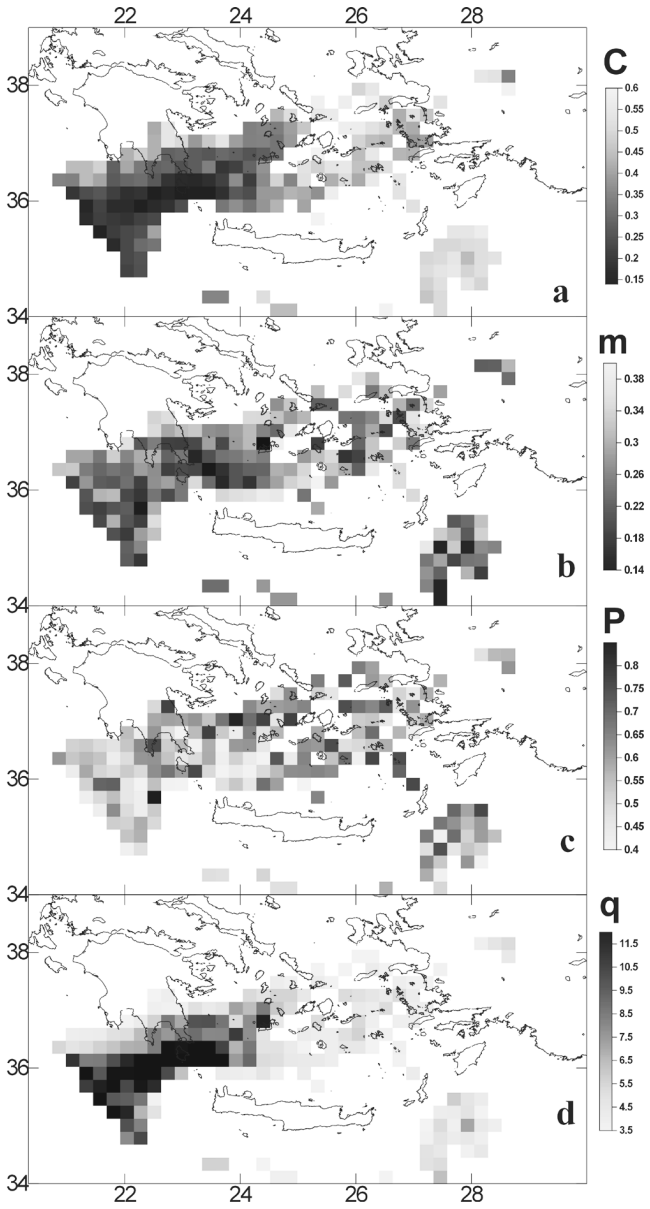

Figure 2. Spatial distribution of parameters (a) C, (b) m, (c) P, and (d) q in the southern Aegean area. Notice the area of very low C- and high q-values in the broader Cythera area.

that the region of accelerated deformation defined for the proposed earthquake epicenter has a similar orientation and spatial extent with the area of very low C and m and high P- and q-values of Figure 2. The corresponding Benioff-strain variation with time for the region presented in Figure 3 is shown in Figure 4. For comparison the cumulative Benioff-strain release after 1965 for the broader southern Aegean area is shown in Figure 5 for two minimum magnitudes ($M_{\min}$ 5.0 and $M_{\min}$ 4.5) and for the completeness periods corresponding to these minimum magnitudes. It is clearly seen that although a linear strain release with time is observed for the broader southern Aegean, the strain time

Table 1

Epicenter Coordinates (φ_N^0, λ_E^0), Magnitude (M), and Origin Time (t_c) of the Expected Mainshock and Model Parameters of the Best-Accelerated Strain-Release Solution Obtained in the Present Study for the Western Part of the Southern Aegean (Cythera Area)*

$(\varphi_N^0, \lambda_E^0)$	M	t_c	C	m	P	q	a(km)	z	e	M_{min}	n	t_s	Area
36.4° N, 22.8° E	6.8	2002.8	0.15	0.20	0.5	16.5	289	70°	0.95	5.0	34	1959	Cythera
36.5° N, 27.0° E	6.8	2003.5	0.48	0.36	0.5	4.3	289	155°	0.95	5.0	61	1976	SE Aegean

*The indicative solution for the easternmost part of the southern Aegean is also presented.

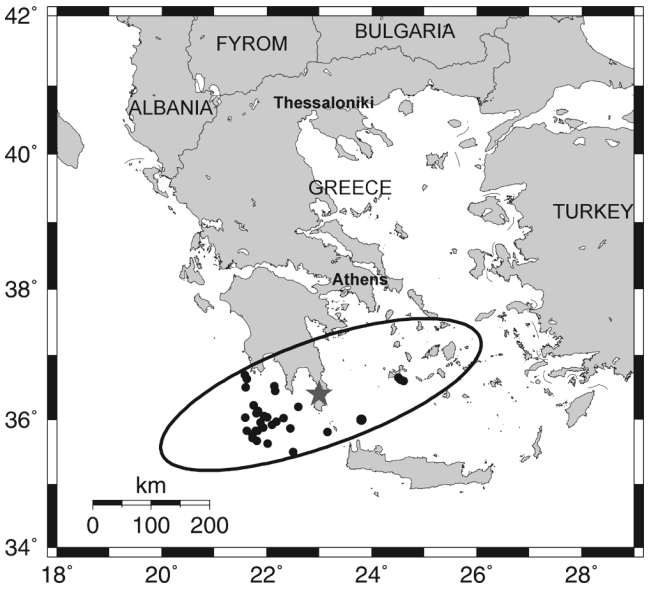

Figure 3. The identified elliptical critical region in the Cythera area and the corresponding preshock epicenters. The epicenter of the expected earthquake is denoted by a star.

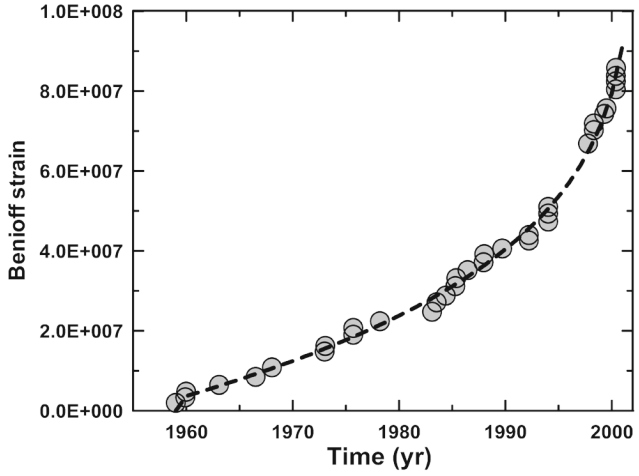

Figure 4. Time variation of the cumulative Benioff strain, $S(t)$, for the Cythera area case studied in this article (M_{min} 5.0). The dashed curve denotes the proposed power-law relation (equation 2). The superiority of the power-law relation compared to a linear fit in describing the strain variation with time is quite clear.

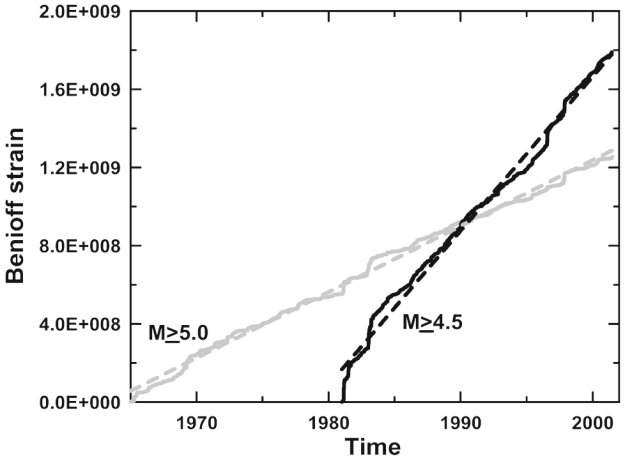

Figure 5. Same as Figure 4 for the whole broader southern Aegean area, using two minimum magnitude values (5.0 and 4.5) for the corresponding completeness periods. No acceleration of the Benioff strain release can be identified.

variation is clearly significantly accelerating for the proposed preshock region.

Figure 6 shows the time variation of the parameter C, calculated using the same data as in Figures 3 and 4, without considering the mainshock magnitude. For this purpose, the first six preshocks of the critical region were considered, and all parameters of equation (2) and the curvature parameter, C, were calculated by considering the determined occurrence time, t_c, for the mainshock. The number of shocks was gradually increased until their total number within the critical region was reached. The value of C continuously decreases as the origin time of the mainshock is approached. A similar variation of C was observed before strong earthquakes in the broader Aegean area (Karakaisis *et al.,* 2002).

Figure 7 shows the time variation of the parameter b of the Gutenberg and Richter (1944) recurrence law, using the same data as in Figures 3 and 4. The b-values were calculated for a moving window of at least 40 preshocks, with a step of one preshock, under the constraint that the magnitude range (denoted by the dashed line) was at least 1.5 (Papazachos, 1974a). Both constrains (minimum number of events and magnitude range) were used in order to avoid instabilities in the b-value estimation. A strong decrease of the b-value is observed for the same elliptical preshock region. Such a significant decrease of b has also been observed be-

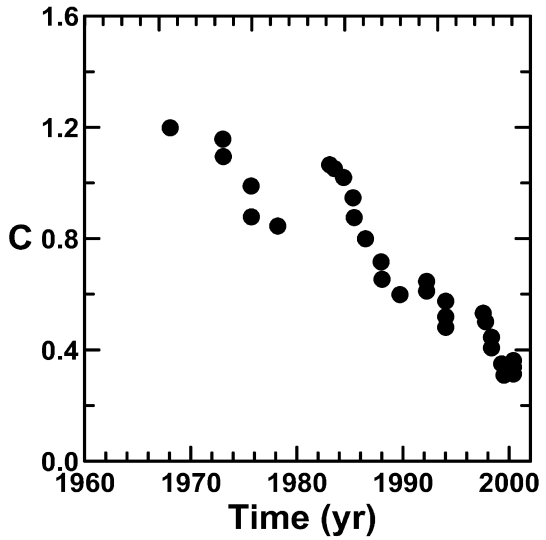

Figure 6. Time variation of the *C*-value from 1967 to present for the critical region identified in the Cythera area. A rapid decrease of the *C*-value can be identified (see text for explanation).

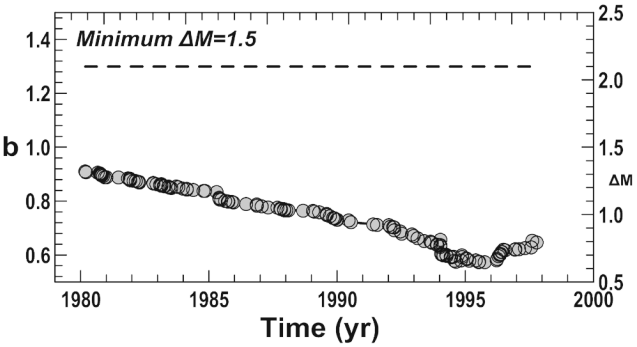

Figure 7. Time variation of the *b*-value from 1980 up to present for the critical region identified in the Cythera area (see text for explanation), using a minimum magnitude range of $\Delta M = 1.5$ for the estimation of the Gutenberg–Richter curve parameters. A decrease similar to *C* is also observed.

fore mainshocks in the Aegean area (Karakaisis *et al.,* 2002) and is expected for regions approaching criticality (Jaume and Sykes, 1999).

Estimation of Uncertainties

The estimation of uncertainties is an inherent part of the whole procedure for earthquake prediction. A possible approach to estimate the uncertainties in the predicted epicenter, magnitude, and origin time by the aforementioned method is to retrospectively apply it to events that have already occurred in order to compare predicted and observed parameters. Such retrospective predictions have been performed for 18 shallow mainshocks that occurred in the Aegean area since 1950. This sample includes all $\mathbf{M} \geq 7.0$ events, as well as all events with $6.9 \geq \mathbf{M} \geq 6.0$ since 1980. The application of this procedure (Papazachos *et al.,* 2002) shows that the distance between the predicted and observed epicenter varies between 20 and 100 km, with a mean distance of 65 $\pm$ 28 km. The mean corresponding difference of occurrence (origin) time is almost zero, with a standard deviation of 0.77 yr, while the magnitude bias varies between -0.5 and 0.4, with a zero mean and a standard deviation of 0.23 yr. Hence, we can conclude that the proposed estimates have an uncertainty of 100 km for the epicentral coordinates, less than 1.5 yr for the origin time and up to 0.5 for the magnitude, with a high (2σ/90%) confidence.

However, retrospective analysis is not enough for a complete evaluation of the uncertainties involved in the proposed prediction. We also have to check our results for the possibility that the identified accelerated seismic deformation pattern could also have occurred for a random data set. This test can be easily performed by applying the proposed detection method on synthetic random catalogs, as also suggested by Bowman *et al.* (1998) and Zoller *et al.* (2001). Using this approach, we can assess the probability that the obtained results either reflect the underlying critical point process or are due to the data randomness and the large parametric space examined for the critical area (e.g., ellipticity, azimuth, size, duration of preshock period, etc.).

In order to create synthetic but also realistic random catalogs, we have adopted the following procedure that has the same steps but different approach as that by Zoller *et al.* (2001):

1. The original earthquake catalog ($M \geq 4.5$) is initially declustered from its aftershocks. For the aftershock sequence duration we use the results of Papazachos (1974b,c) and Papazachos and Papazachou (1997), whereas for the aftershock area we used a circular region with a radius, *R*, given by

$$\log R = 0.19\mathbf{M} + 0.36, \tag{13}$$

   which was defined by the use of all aftershocks sequence in Greece and surrounding area.
2. On the basis of the declustered catalog and the application of Poisson time distribution for the occurrence times and the Gutenberg–Richter equation for the magnitude distribution of each seismogenic zone defined for the Aegean area (Papaioannou and Papazachos, 2000), we estimated the corresponding random epicenter distributions in space and time, which are in this way fit (equivalent) to the declustered catalog.
3. Aftershocks following the time pattern proposed by Mogi (1962) and adapted by Papazachos (1974c) for the Aegean area, and equation (13), for their spatial distribution were added to the random catalogs to calculate the final synthetic catalogs.

We should point out that rectangular or elliptical regions having the direction of the main event fault zone would be

more appropriate than a circular region (equation 13) for the aftershock area. For the Aegean area, however, fault-zone information is not always available, nor is it possible to use such regions for stage 3 of the process, where aftershocks for random mainshocks are added back to the earthquake catalog.

In order to test the efficiency of the proposed algorithm we have applied the same procedure on a large number of random catalogs. For this reason, we examined the grid of points (spacing 0.25°) in the southern Aegean area that consists of ~800 search points. The results obtained for the synthetic catalogs were quite surprising: approximately 15% of the points examined exhibited accelerated seismicity patterns in accordance with the criteria defined by equations (3)–(7) and (9). This observation suggests that it is possible to identify areas, which falsely appear to be under a state of accelerated deformation, even when the underlying seismicity distribution is random in time and space. Figure 8 presents the spatial distribution of the *C*- and *q*-values in the examined area for two random catalogs using the same gray scale as in Figure 2 for comparison.

Although the results previously obtained seem at a first glance to be disappointing for the robustness and reliability of the prediction proposed, a careful examination of the determined *C*-, *m*-, *P*-, and *q*-values of the observed and synthetic catalog results suggests a different situation. The first remark is that from the observed catalog we have obtained solutions for approximately 25% of the examined points, which is quite higher than the 15% found (on the average) for synthetic catalogs and higher than the number of solutions obtained for any of the synthetic catalogs tested. Figure 9 shows the frequency histograms of the *C*-, *m*-, *P*-, and *q*-values obtained for all the random catalogs tested. On the same plot, the solutions obtained for the observed catalog in the Cythera area corresponding to the best solution (solid arrow) and the average of the five best grid solutions (open arrow), all located in the Cythera area, are shown. It is clearly observed that although the random solutions show similar *m*- and *P*-values with the solutions obtained from the observed catalog, there are no random solutions with as small *C*-values or as large *q*-values.

The interpretation of Figure 9 is straightforward: using a synthetic random catalog it is possible to misidentify false strong accelerated deformation behavior (small *m*-values), which are compatible with the strict constrains set by equations (3)–(7) describing this accelerated pattern behavior (high *P*-values). However, the solutions obtained for the Cythera area show a much higher compatibility of the Benioff strain time evolution with equation (2) (small *C*) than with any random catalog. Furthermore, the random solutions exhibit much lower *q*-values compared to the solutions for the Cythera area. Figure 9d reveals the usefulness of parameter *q*: solutions from random catalogs can exhibit low *m*-, high *P*-, or relatively low *C*-values, as is the case with so-called real accelerated deformation for observed events. However, it is not possible to exhibit this behavior simultaneously, as

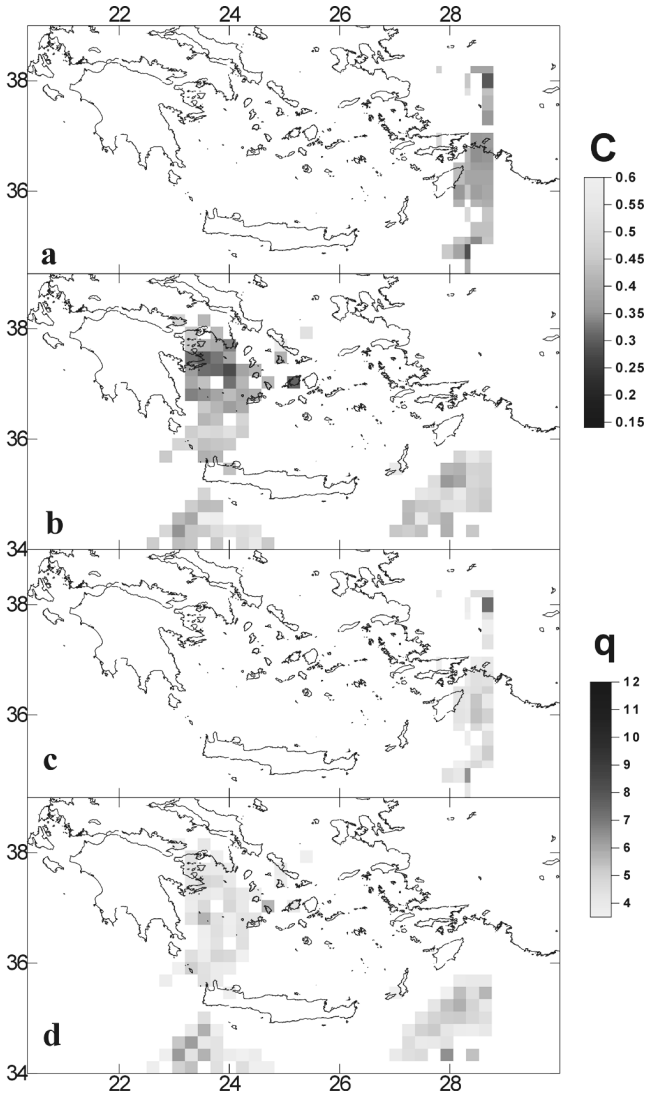

Figure 8. Spatial variation of parameters *C* (a, b) and *q* (c, d) for two of the random catalogs used in the present study. The gray scale is the same as in Figure 2.

is seen by Figure 9d, where 88% of random-catalog solutions have a *q*-value less than 6 and no *q*-value exceeds 10. Therefore, on the basis of these results, as well as of the previous analysis, we can expect that the proposed mainshock will occur within a circle of 100 km from the proposed position (36.4° N, 23.0° E), with **M** 6.8 ± 0.5 in the time interval (yr) 2001.3–2004.3.

The spatial distribution of the obtained solutions (see Fig. 2) is not only limited to the Cythera area, but solutions are also found for the easternmost part of the southern Aegean area. The solutions in this area correspond to different critical regions, located in the easternmost Greek islands (Samos, Cos, and Rhodes) and the coasts of Asia Minor. Examination of the best solutions (Fig. 2) shows that the solutions tend to cluster in two areas, one just north of the Cos island (37.30° N, 26.40° E, $h \leq 100$ km, corresponding to **M**

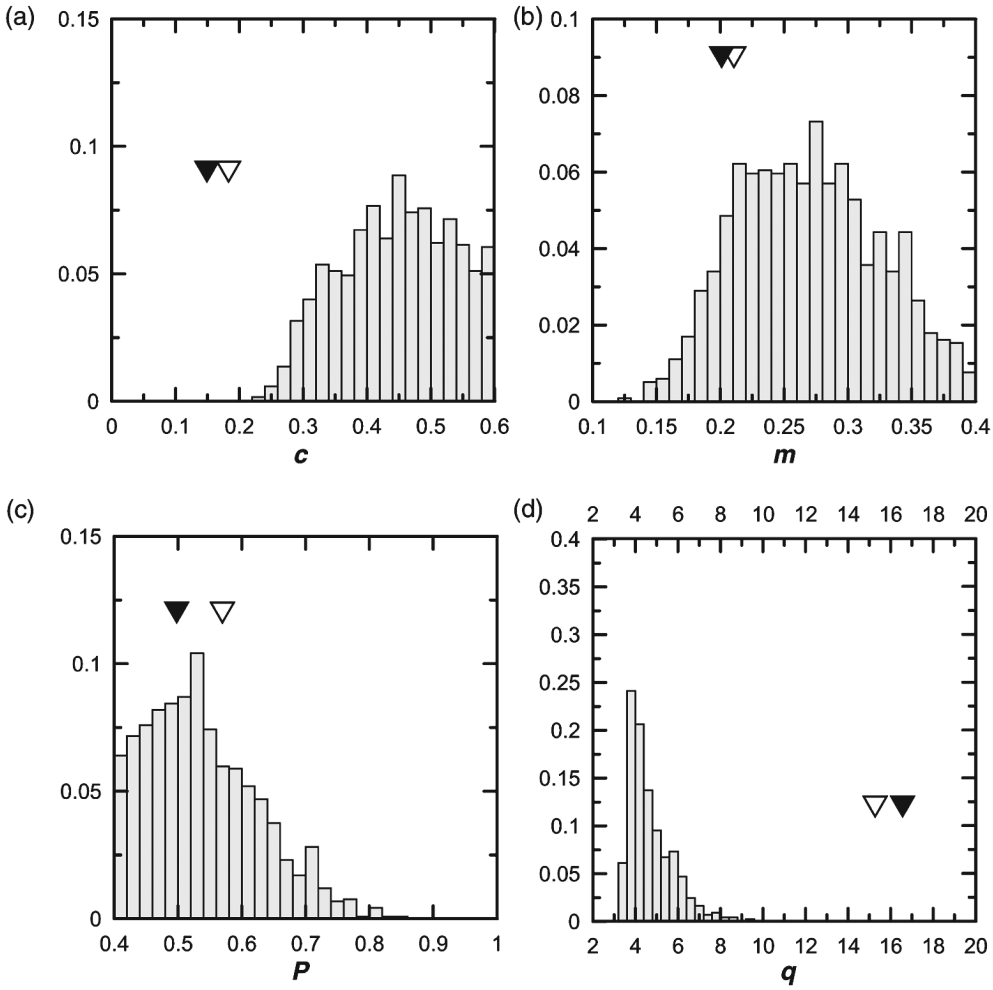

Figure 9. Frequency histogram of the distribution of parameters (a) C, (b) m, (c) P, and (d) q of the solutions (erroneous observations of accelerated seismic deformation) obtained using synthetic random catalogs for the study area. Notice the significant deviation from the random catalog distribution of the C- and q-values derived from the observed catalog, which are denoted by solid (best solution maximum q) and solid triangles (average of 5 best largest q solutions).

6.7) and one along the external Hellenic Arc, south of the Rhodes island (35.50° N, 27.70° E, $h \leq 100$ km, corresponding to **M** 6.6), with some solutions spatially located between the two clusters. Examination of the parameters of the corresponding solutions (azimuth of the critical areas, etc.) shows that the solutions north of Cos seem to be located along the extention of the Cythera anomaly. On the other hand, all solutions south of Cos have preshock areas with an orientation of approximately 150°, covering the whole eastern part of southern Aegean. It is very difficult to propose a strategy in identifying the right solution, if any, given the observed q-values (~4–5.5) of the corresponding solutions in comparison to some high q solutions of the random catalogs.

Figure 10 shows the observed Benioff-strain acceleration for the grid point 36.50° N, 27.00° E. We decided to show results for this point because the corresponding elliptical critical region includes most of the eastern part of southern Aegean, including both high-q clusters north of Cos and south of Rhodes. Furthermore the determined solution is based on a large number of events (more than 60) and the critical region properties (ellipticity, orientation, etc.) are similar, hence representative, with most solutions in the eastern part of southern Aegean. The acceleration model parameters are listed in second line of Table 1, and they correspond to a **M** 6.8 mainshock in the eastern Aegean. Although the acceleration pattern seen in Figure 10 is quite clear, the lower q-values (compared to the Cythera case) suggest that a careful monitoring and re-estimation of the model parameters is necessary in the near future in order to verify and evaluate the evolution of the accelerated deformation behavior in the eastern part of the southern Aegean area.

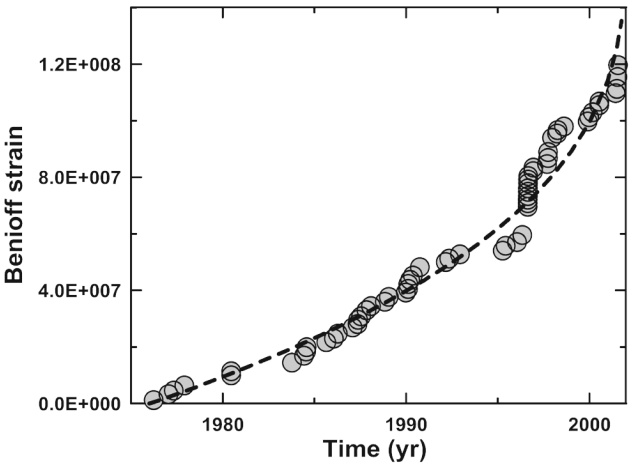

Figure 10. Time variation of the cumulative Benioff strain, $S(t)$, for the eastern part of the southern Aegean area. A clear acceleration of the Benioff strain with time is also observed for this case, similar to Figure 4.

Discussion

The main target of the present article is to investigate the properties of the active part of the lithosphere in the southern Aegean area (34° N–38.5° N, 19° E–30° E). It has been shown that during the last three decades the seismic crustal deformation (expressed by the cumulative Benioff strain) is accelerating in an elliptically shaped region in the southwestern Aegean. Several properties of the observed seismic deformation are very similar to properties of preshock regions that have been identified for other strong (**M** ≥6.0) shallow earthquakes in the Aegean area, expressed by equations (2)–(9). Tests through synthetic but realistic random catalogs suggest a possibility of 15% for misidentification of an area, which falsely exhibits an accelerated seismic deformation pattern compatible with these equations. In only 12% of these cases, therefore 1.8% of the total number of cases, q-value (which is a general measure of the compatibility of the accelerated deformation model) exceeds 6. Furthermore, the observation that C and q obtained for the Cythera area are clearly outside the limits defined by solutions obtained from random catalogs suggests that it is extremely unlikely that the obtained acceleration pattern is a random feature.

The results of the present work can contribute to the research for intermediate-term earthquake prediction. The occurrence of a mainshock in this region with the estimated space, time, and magnitude windows will be strong evidence that the method applied in the present work can be effectively used for such prediction of certain crustal events. In the opposite case, it will suggest that such behavior can be observed without any connection to precursory phenomena. In any case, the effectiveness of the proposed method can only be assessed by statistical application to various cases and areas. A retrospective analysis of the space-time behavior of accelerated deformation patterns through the last 50 yr, which is currently under preparation, might help to identify such cases and assess the possibility for a future repetition of such phenomena.

The area of the southern Aegean (southern part of the Hellenic arc), where the mainshock (or mainshocks) is expected to occur, has been repeatedly struck by earthquakes of a similar order of magnitude (M_w ≥6.8). Between 1840 and 1957 26 such events have occurred in the southernmost part of the Aegean (34–37° N, 21–30° E), with a maximum interevent time of less than 30 yr. However, since 1957 no such mainshock has occurred in this area (Papazachos and Papazachou, 1997; Papazachos *et al.,* 2000a). The lack of large earthquake activity for more than 40 yr in an area of high active deformation strongly suggests that it is an earthquake-prone area. This observation supports the results of the present work: large events are expected during the next few years, as it is concluded from the space-time distribution of intermediate-magnitude events.

If we consider the possible effect of these M_W ≥6.8 events, we should point out that some of these earthquakes were associated with strong tsunamis, hence a tsunami could also result from the proposed earthquake in the western part of the southern Aegean. However, the last large earthquake in this area, which occurred on 11 August 1903 (**M** 7.4), was not associated with strong tsunami, probably due to its large focal depth. On the other hand, it caused severe damage not only in Cythera island but also on the Greek mainland (southern Peloponnesus). Therefore, similar effects can be expected as a result of the proposed future earthquake in all of the surrounding area (Cythera, south Peloponnese, western Crete, western Cyclades islands). Independently of the occurrence in the near future of the proposed earthquakes, the observations show that the broader southern Aegean area, and especially its southwestern part, is seismically in an excitation state. As a result, the occurrence of intermediate magnitude strong earthquakes (with magnitude ~6.0), which can also cause damage in this area, should also be considered as very probable.

Acknowledgments

We would like to thank D. Bowman, A. Mitchel, and an anonymous reviewer for their constructive criticism and valuable suggestions. We thank Wessel and Smith (1995) for their generous distribution of the Generic Mapping Tools software, which was used to generate some of the figures in this article. This work has been partly financed by the Greek Earthquake Planning and Protection Organization (OASP) under project 20239, Aristotle University Thessaloniki Research Committee.

References

Bowman, D. D., G. Ouillon, C. G. Sammis, A. Sornette, and D. Sornette (1998). An observational test of the critical earthquake concept, *J. Geophys. Res.* **103,** 24,359–24,372.

Bufe, C. G., and D. J. Varnes (1993). Predictive modelling of seismic cycle of the Great San Francisco Bay Region, *J. Geophys. Res.* **98,** 9871–9883.

Bufe, D. G., S. P. Nishenko, and D. J. Varnes (1994). Seismicity trends and potential for large earthquakes in the Alaska-Aleutian region, *Pure Appl. Geophys.* **142,** 83–99.

Gutenberg, B., and C. F. Richter (1944). Frequency of earthquakes in California, *Bull. Seism. Soc. Am.* **34,** 185–188.

Huang, Y., H. Saleur, C. Sammis, and D. Sornette (1998). Precursors, aftershocks, criticality and self organized criticality, *Europhys. Lett.* **41,** 43–48.

Jaume, S. C., and L. R. Sykes (1999). Evolving towards a critical point: a review of accelerating seismic moment/energy release rate prior to large and great earthquakes, *Pure Appl. Geophys.* **155,** 279–306.

Karakaisis, G. F., M. C. Kourouzidis, and B. C. Papazachos (1991). Behavior of the seismic activity during a single seismic cycle, in *International Conference on Earthquake prediction: State-of-the-Art,* Strasbourg, France, 15–18 October 1991, 47–54.

Karakaisis, G. F., A. S. Savvaidis, and C. B. Papazachos (2002). Time variation of parameters related to the accelerating preshock crustal deformation in the Aegean area, *Pure Appl. Geophys.* (in press).

Knopoff, L., T. Levshina, V. J. Keilis-Borok, and C. Mattoni (1996). Increased long-range intermediate-magnitude earthquake activity prior to strong earthquakes in California, *J. Geophys. Res.* **101,** 5779–5796.

Mogi, K. (1962). On the time distribution of aftershocks accompanying the recent major earthquakes in and near Japan, *Bull. Earthquake Res. Inst. Univ. Tokyo* **40,** 107–124.

Mogi, K. (1969). Some features of the recent seismic activity in and near Japan. II. Activity before and after great earthquakes, *Bull. Earthquake Res. Inst. Univ. Tokyo* **47,** 395–417.

Papadopoulos, G. A. (1986). Long term earthquake prediction in western Hellenic arc, *Earthquake Pred. Res.* **4,** 131–137.

Papaioannou, Ch., and B. C. Papazachos (2000). Time-independent and time-dependent seismic hazard in Greece based on seismogenic sources, *Bull. Seism. Soc. Am.* **90,** 22–33.

Papazachos, B. C. (1974a). Dependence of the seismic parameter b on the magnitude range, *Pure Appl. Geophys.* **112,** 1059–1065.

Papazachos, B. C. (1974b). On certain foreshock and aftershock parameters in the area of Greece, *Annali Geofisica* **27,** 497–515.

Papazachos, B. C. (1974c). On the time distribution of aftershocks and foreshocks in the area of Greece, *Pure Appl. Geophys.* **112,** 627–631.

Papazachos, B. C. (1990). Seismicity of the Aegean and surrounding area, *Tectonophysics* **178,** 287–308.

Papazachos, B. C., and C. C. Papazachou (1997). *Earthquakes of Greece,* Ziti Publ., Thessaloniki, 304 pp.

Papazachos, B. C., and C. B. Papazachos (2000). Accelerated preshock deformation of broad regions in the Aegean area, *Pure Appl. Geophys.* **157,** 1663–1681.

Papazachos, B. C., P. E. Comninakis, G. F. Karakaisis, B. G. Karakostas, Ch. A. Papaioannou, C. B. Papazachos, and E. M. Scordilis (2000a). *A Catalogue of Earthquakes in Greece and Surrounding Area for the Period 550 B.C.–1999,* Publ. Geoph. Lab., Univ. of Thessaloniki.

Papazachos, B. C., G. F. Karakaisis, C. B. Papazachos, A. C. Savvaidis, and E. M. Scordilis (2000b). Properties of the preshock crustal deformation in the region of the Aegean area, in *Proc. of the 27th General Assembly of the European Seismological Community,* Lisbon, Portugal, 10–15 September 2000, 295–300.

Papazachos, B. C., G. F. Karakaisis, C. B. Papazachos, E. M. Scordilis, and A. S. Savvaidis (2001). A method for estimating the origin time of an ensuing mainshock by observations of preshock crustal seismic deformation, in *Proc. 9th International Congress Geol. Soc. Greece,* Athens, *20–25 September 2001,* Vol. 4, 1573–1582.

Papazachos, C. B., and B. C. Papazachos (2000). Observations on preshock seismic deformation in the Aegean area and earthquake prediction, in *Proc. of the 27th General Assembly of the European Seismological Community,* Lisbon, Portugal, 10–15 September 2000, 301–305.

Papazachos, C. B., and B. C. Papazachos (2001). Precursory seismic deformation in the Aegean area, *Ann. Geofisica* **144,** 461–474.

Papazachos, C. B., G. F. Karakaisis, and E. M. Scordilis (2002). Results of a retrospective prediction of past strong mainshocks in the broader Aegean area by application of the accelerating seismic deformation method, *Pure Appl. Geophys.* (submitted).

Sornette, A., and D. Sornette (1990). Earthquake rupture as a critical point. Consequences for telluric precursors, *Tectonophysics* **179,** 327–334.

Sornette, D., and C. G. Sammis (1995). Complex critical exponents from renormalization group theory of earthquakes: implications for earthquake predictions, *J. Phys. I. France* **5,** 607–619.

Sykes, L. R., and S. Jaume (1990). Seismic activity on neighboring faults as a long term precursor to large earthquakes in the San Francisco Bay area, *Nature* **348,** 595–599.

Tocher, D. (1959). Seismic history of the San Francisco bay region, *Calif. Div. Mines Spec. Rep. 57,* 39–48.

Tzanis, A., F. Vallianatos, and K. Makropoulos (2000). Seismic and electric precursors to the 17–1–1983, M 7 Kefallinia earthquake, Greece: signatures of a SOC system, *Phys. Chem. Earth* **25,** 281–287.

Varnes, D. J. (1989). Predicting earthquakes by analyzing accelerating precursory seismic activity, *Pure Appl. Geophys.* **130,** 661–686.

Vere-Jones, D., R. Robinson, and W. Yang (2001). Remarks on the accelerated moment release model: problems of model formulation, simulation and estimation, *Geophys. J. Int.* **144,** 517–531.

Wessel, P., and W. Smith (1995). New version of the Generic Mapping Tools, *EOS,* 76–329.

Yang, W., D. Vere-Jones, and M. Li (2001). A proposed method for locating the critical point of a future earthquake using the critical earthquake concept, *J. Geophys. Res.* **106,** 4121–4128.

Zoller, G., S. Hainzl, and J. Kurths (2001). Observation of growing correlation length as an indicator for critical point behavior prior to large earthquakes, *J. Geophys. Res.* **106,** 2167–2175.

Geophysical Laboratory
School of Geology
University of Thessaloniki
Thessaloniki, Greece
costas@lemnos.geo.auth.gr
karakais@geo.auth.gr
alekos@lemnos.geo.auth.gr
basil@lemnos.geo.auth.gr

Manuscript received 31 July 2000.